Quantitative determination of singlet oxygen density and temperature for Oxygen-Iodine Laser Applications

Manish Gupta [a,*], Thomas Owano [a], Douglas S. Baer [a],
Anthony O'Keefe, Skip Williams [b,*]

[a] *Optical Division, Los Gatos Research, Inc., 67 East Evelyn Ave, Suite 3, Mountain View, CA 94041, USA*
[b] *Air Force Research Laboratory, Space Vehicles Directorate, 29 Randolph Road, Hanscom AFB, MA 01731-3010, USA*

Abstract

The absolute density of singlet oxygen has been quantitatively determined using off-axis integrated cavity output spectroscopy to measure the Q(2)–Q(18) lines of the (0,0) band of the $b^1\Sigma_g^+ \leftarrow a^1\Delta_g$ Noxon system near 1910 nm. Using derived values for the absorption cross-sections and a fitted rotational temperature of 295 K, a singlet oxygen density of 3×10^{15} molecules cm^{-3} (5% conversion efficiency) was obtained in the afterglow of a 13.56 MHz RF discharge. The observed line spectrum for the Q(12) transition has a signal-to-noise ratio of 120:1 signifying that singlet oxygen densities as low as 2.5×10^{13} molecules cm^{-3} are detectable.
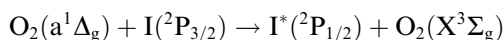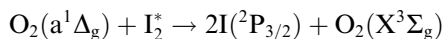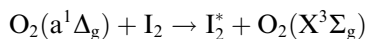© 2004 Elsevier B.V. All rights reserved.

1. Introduction

Lasing in the Chemical Oxygen-Iodine Laser (COIL) occurs at 1.315 μm via a stimulated emission of excited iodine atoms [1].

$$I^*(^2P_{1/2}) + h\nu \rightarrow I(^2P_{3/2}) + 2h\nu$$
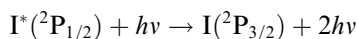
The excited $I^*(^2P_{1/2})$ atoms are generated from iodine molecules in a series of steps involving $O_2(a^1\Delta_g)$.

$$O_2(a^1\Delta_g) + I_2 \rightarrow I_2^* + O_2(X^3\Sigma_g)$$

$$O_2(a^1\Delta_g) + I_2^* \rightarrow 2I(^2P_{3/2}) + O_2(X^3\Sigma_g)$$

$$O_2(a^1\Delta_g) + I(^2P_{3/2}) \rightarrow I^*(^2P_{1/2}) + O_2(X^3\Sigma_g)$$

After including other possible deactivation steps, it has been estimated that approximately 5 $O_2(a^1\Delta_g)$ are required to transform a single I_2 molecule into 2 $I^*(^2P_{1/2})$

atoms [2]. Therefore, the efficiency and power of COIL are greatly dependent on the amount of $O_2(a^1\Delta_g)$ present in the laser. Much effort in COIL development has gone towards finding more efficient and less hazardous methods of producing large densities of $O_2(a^1\Delta_g)$ and a variety of schemes have been developed, including wet chemical reactions, electric discharges, optical pumping, and alternate energy transfer methodologies. In order to gauge the utility of these schemes as well as provide an in situ diagnostic of the COIL's performance, it is important to accurately measure the absolute density of $O_2(a^1\Delta_g)$. In addition to this measurement, it is also important to determine the internal state distribution of $O_2(a^1\Delta_g)$, because the efficiency of the aforementioned reactions depends on its rovibrational state. An ideal diagnostic would provide both an accurate, absolute $O_2(a^1\Delta_g)$ density and some measure of its internal state distribution.

Besides COIL, singlet oxygen also plays a vital role in a variety of chemical processes. In the stratosphere and mesosphere, where singlet oxygen densities are largest, it is responsible for one the strongest features of the day and night airglow and significantly effects the radiative

---

* Corresponding authors. Fax: +1 650 965 7074 (M. Gupta); +1 937 255 7292 (S. Williams).
E-mail addresses: m.gupta@lgrinc.com (M. Gupta), skip.williams@wpafb.af.mil (S. Williams).

Report Documentation Page

Public reporting burden for the collection of information is estimated to average 1 hour per response, including the time for reviewing instructions, searching existing data sources, gathering and maintaining the data needed, and completing and reviewing the collection of information. Send comments regarding this burden estimate or any other aspect of this collection of information, including suggestions for reducing this burden, to Washington Headquarters Services, Directorate for Information Operations and Reports, 1215 Jefferson Davis Highway, Suite 1204, Arlington VA 22202-4302. Respondents should be aware that notwithstanding any other provision of law, no person shall be subject to a penalty for failing to comply with a collection of information if it does not display a currently valid OMB control number.

1. REPORT DATE **2004**	2. REPORT TYPE	3. DATES COVERED **00-00-2004 to 00-00-2004**

4. TITLE AND SUBTITLE **Quantitative determination of singlet oxygen density and temperature for Oxygen-Iodine Laser Applications**	5a. CONTRACT NUMBER
	5b. GRANT NUMBER
	5c. PROGRAM ELEMENT NUMBER
6. AUTHOR(S)	5d. PROJECT NUMBER
	5e. TASK NUMBER
	5f. WORK UNIT NUMBER

7. PERFORMING ORGANIZATION NAME(S) AND ADDRESS(ES) **Air Force Research Laboratory,Space Vehicles Directorate,29 Randolph Road,Hanscom AFB,MA,01731-3010**	8. PERFORMING ORGANIZATION REPORT NUMBER

9. SPONSORING/MONITORING AGENCY NAME(S) AND ADDRESS(ES)	10. SPONSOR/MONITOR'S ACRONYM(S)
	11. SPONSOR/MONITOR'S REPORT NUMBER(S)

12. DISTRIBUTION/AVAILABILITY STATEMENT
Approved for public release; distribution unlimited

13. SUPPLEMENTARY NOTES

14. ABSTRACT
see report

15. SUBJECT TERMS

16. SECURITY CLASSIFICATION OF:			17. LIMITATION OF ABSTRACT	18. NUMBER OF PAGES **5**	19a. NAME OF RESPONSIBLE PERSON
a. REPORT **unclassified**	b. ABSTRACT **unclassified**	c. THIS PAGE **unclassified**			

properties of the atmosphere [3]. Because of the importance of these transitions, they are spectroscopically well-characterized and are still the focus of much recent work [4–9].

Several methods have been developed to measure singlet oxygen, including emission spectroscopy [10], tunable diode laser absorption spectroscopy [11], Raman scattering [12], intracavity laser absorption spectroscopy (ICLAS) [13], electron spin resonance (ESR) [14], and resonance enhanced multiphoton ionization (REMPI). However, a straightforward method of quantifying the density and temperature of singlet oxygen is still lacking. In this Letter, we report the application of off-axis integrated cavity output spectroscopy (off-axis ICOS) to address this problem by directly measuring the absorption spectra of singlet oxygen near 1910 nm by exploiting the (0,0) band of the Noxon system ($b^1\Sigma_g^+ \leftarrow a^1\Delta_g$). Our earlier work focused on measuring the overtone (1,0) band of this spectroscopic system around 1505 nm [15], and the two approaches are contrasted below.

2. Experiment

The off-axis ICOS system, shown in Fig. 1, has been described previously [16] and only a brief overview will be provided here. A nitrogen purged, single-mode DFB diode laser providing 4 mW around 1910 nm is coupled into a 0.8-m long, high-finesse cavity comprised of two highly reflective mirrors ($R = 99.9159\%$) in an off-axis fashion. The latter alignment helps suppress optical interference by making the laser beam trace several hundred passes within the cavity before overlapping itself. In cavity enhanced absorption measurements, the total effective pathlength, L_{eff}, traveled by the light is typically

between 1 and 100 km and is given by $L_{eff} = L*R/(1-R)$, where L is the cavity length and R is the mirror reflectivity. Light transmitted through the cavity is focused onto an amplified TE-cooled extended-InGaAs detector (responsivity of 1.1 A/W at 1910 nm). In order to reduce the background detector noise, the extended-InGaAs element is maintained at -24.9 °C.

The effective pathlength of the cavity used in the present work ($L_{eff} = 972$ m) was measured by cavity ringdown spectroscopy [17] and confirmed by measuring an overtone absorption of pure carbon dioxide at 5231.566 cm^{-1} and utilizing its published linestrength in the HITRAN database [18]. The laser is currently tuned approximately 30 GHz over the singlet oxygen absorption feature of interest and then temperature-tuned between 5229 and 5239 cm^{-1} in order to measure the Q(2)–Q(18) lines. The precise spectral position of the laser is determined by measuring previously identified water absorptions (HITRAN database [18]) in ambient air combined with simultaneously recorded etalon transmission traces (FSR = 2.0 GHz).

Singlet oxygen is generated in a 13.56 MHz radio-frequency inductively-coupled plasma (RF-ICP) by flowing 10% O_2/He through a 25-mm diameter quartz tube and coupling 270 W of RF power into the gas. The plasma afterglow is flowed through the measurement cell at approximately 3000 SCCM at a total pressure of 20 Torr. In order to minimize the collisional deactivation of singlet oxygen, the optical cell and all associated fittings are quartz coated.

3. Results and discussion

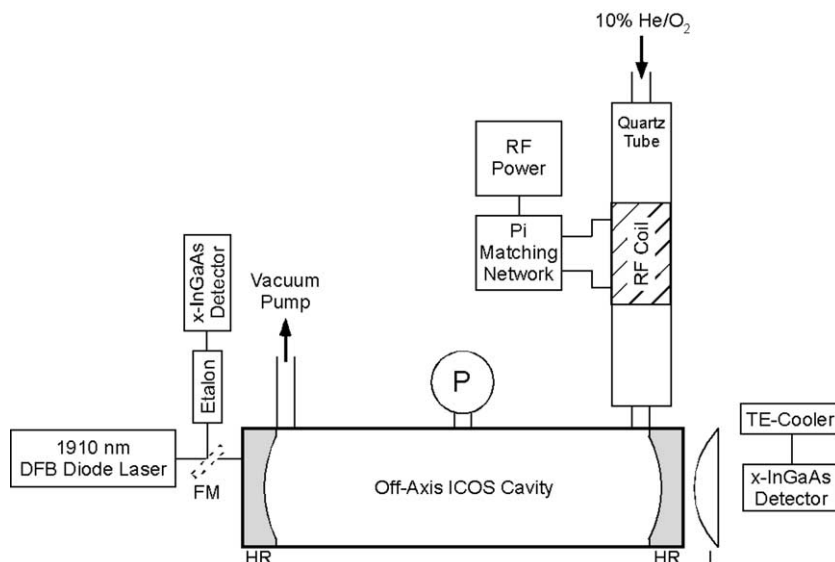The measured cavity-enhanced spectra of the Q(2)–Q(18) absorption features are shown in Fig. 2, and all

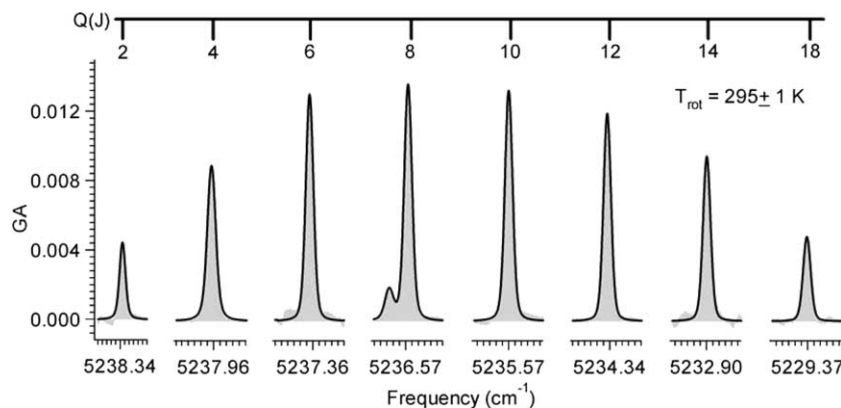Fig. 1. Off-axis ICOS experimental setup.

Fig. 2. Measured (gray) singlet oxygen Q-branch absorption features fit to Voigt profiles (black). All eight lines were fit to a single rotational temperature with independent Lorentzian components. The absolute frequency axis was calibrated using known water transitions and an etalon, and the absorption features are within 0.01 cm^{-1} of their predicted location.

singlet oxygen lines are found to be within 0.01 cm^{-1} of their predicted positions. Due to strongly absorbing water lines, the Q(16) feature is completely obscured and the Q(8) line fit must include an overlapping water line. The entire Q-branch spectrum is simultaneously fit with Voigt lineshapes sharing a common Doppler width, but varying Lorentzian components. The line strengths are taken from Chiu [19] and only the temperature and individual Lorentzian widths are adjustable in the fit. The Lorentzian width is four times smaller than the Doppler (Gaussian) width and only varied by ±10% over the entire spectrum, well within the fit error. The fit yields a temperature of 295 ± 1 K, consistent with expectations.

A high-resolution Voigt fit of the measured Q(12) transition is shown in Fig. 3 and yields Gaussian and Lorentzian full-width-half-maximums of 0.01141 and 0.0027 ± 0.0002 cm^{-1}, respectively. The former gives a translational temperature of 298 ± 2 K, in excellent agreement with that determined by simultaneously fitting the Q-branch transitions. The Lorentzian full width

is ascribed to collisional band broadening (pressure broadening). No studies have been performed that report the pressure-induced shifts and widths of these lines. However, some recent detailed studies involving the $b^1\Sigma_g^+ \leftarrow X^3\Sigma_g^-$ atmospheric [7,20] and $a^1\Delta_g \leftarrow X^3\Sigma_g^-$ IR atmospheric [6,7] bands have been reported. These studies were performed at pressures ranging from ~100 to ~760 Torr. Assuming that the broadening of the $b^1\Sigma_g^+ \leftarrow a^1\Delta_g$ (0,0) band can be taken as the average of these two bands and that the experimental results can be extrapolated down to our 20 Torr experimental pressure, the rotational level average values reported by Cheah et al. [7] yield a Lorentzian width of 0.0020 cm^{-1}. Similarly, Brown and Plymate [20] and Newman et al. [6] derived rotational level specific broadening coefficients for the $b^1\Sigma_g^+ \leftarrow X^3\Sigma_g^-$ (0,0) and $a^1\Delta_g \leftarrow X^3\Sigma_g^-$ (0,0) bands, respectively. These coefficients yield a value of 0.0024 cm^{-1} for the Lorentzian full width of the Q(12) transition due to pressure broadening.

Note that the pressure broadening coefficients above are for O_2 and N_2, which have nearly identical pressure broadening coefficients. The bulk of the gas used in our experiments is helium for which there is limited data. In one study of the of the pressure broadening of the 118.750 GHz oxygen transition, Setzer and Pickett [21] found that the pressure broadening coefficient for this pure rotation ground state $X^3\Sigma_g^-$ N = 7 ← 6 line for collisions with helium to be 75% that of O_2 and N_2 This result suggests that the value measured under our conditions should be less than the estimates given above. Therefore, the observation 0.0027 cm^{-1} for the Lorentzian width of the observed Q(12) transition is in general agreement with the available data but larger than expected based on reasonable assumptions. Further studies measuring the pressure broadening of these transitions are needed to fully resolve this issue.

In order to deduce the absolute density of singlet oxygen from the cavity-enhanced absorption spectrum, it is
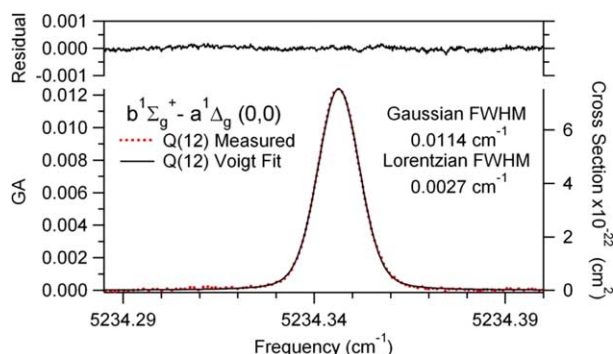

Fig. 3. Cavity-enhanced spectrum (GA) of the Q(12) transition of singlet oxygen. The measured data (circles) is fit to a Voigt profile (solid line), yielding the residual shown atop the figure. The theoretical cross-section for the transition is depicted on the right axis.

necessary to obtain the transition probability. Unlike the oxygen atmospheric and IR atmospheric bands, the absorption cross-sections for the $b^1\Sigma_g^+ \leftarrow a^1\Delta_g$ transition have never been measured individually. The only available experimental data is that of Noxon [22] who reported an absolute transition probability of the b–a, (0,0) transition of 2.5×10^{-3} s^{-1} based on a measured relative intensity of the b–a, (0,0) to b–X, (0,0). In photon units of intensity, the ratio of b–a, (0,0) to b–X, (0,0) was about 0.004 and is accurate to within a factor of two. Using the best values for the b–X, (0,0) transition probability at the time (1961), Noxon derived the absolute transition probability of the b–a, (0,0) to be 2.5×10^{-3} s^{-1}. Currently, the most commonly used probability [23] is based on a value of A for the b–X, (0,0) deduced by Burch and Gryvnak [24] of 1.7×10^{-3} s^{-1}. More recent work (2000) on the transition probability of the b–X, (0,0) transition performed by Cheah et al. [7] yields a value for the b–a, (0,0) of 1.6×10^{-3} s^{-1}.

However, a correction should be made at this point based on the Q-branch intensity. Noxon observed a 70-Å wide feature, superimposed on a strong continuum. In order to estimate the absolute transition probability for the b–a (0,0) band based solely on this observation, Noxon assumed that this feature essentially encompassed the Q-branch of the b–a (0,0) band and that the Q-branch represented one fifth of the total band intensity. Considering the line-strength factors derived by Chiu [19] and verified by Fink et al. [25], the Q-branch actually represents approximately one third of the band intensity. Therefore, the value reported by Noxon should be multiplied by a factor of 3/5 yielding a transition probability of 1×10^{-3} s^{-1}. This revised value is the only experimentally derived value for this transition and has a reported accuracy of a factor of two corresponding to a range of $0.5–2 \times 10^{-3}$ s^{-1}.

Ab initio calculations have been performed to determine these values more accurately. The rovibrational Schrödinger equation has been solved in the case-b limit and excellent agreement with the vibrational energies of the oxygen potential energy surfaces has been obtained. These calculations were then used to solve for the quadrupole transition probability and a value of 1.26×10^{-3} s^{-1} has been calculated [15]. The transition probability is then used to calculate a peak absorption cross-section shown in Fig. 3 using standard formulae [26]. Note that, due to the high certainty with which the low-lying oxygen potential energy surfaces (X, a, and b) are known, the absorption cross-section can be very accurately determined for low vibrational states, and this value is estimated to be accurate to within 5%.

Using the data shown in Fig. 3 and the theoretically obtained cross-section described above, the concentration of singlet oxygen in the $v = 0$, $J = 12$ rovibrational level is 2×10^{14} molecules cm^{-3}. Taking into account that the rotational temperature is 295 K (Fig. 2), and

assuming that the singlet oxygen is rotationally equilibrated (with no significant vibrationally-excited population), the total density of singlet oxygen is 3×10^{15} molecules cm^{-3}. Since the plasma is operated with 2 Torr of oxygen (20 Torr of a 10% O_2/He mix) and 0.09 Torr is converted to singlet oxygen, the plasma conversion efficiency is ~5%. Moreover, the Q(12) line is measured with a S/N ratio of 120:1 after only 100 s of data averaging, giving a minimum detectable singlet oxygen density as low as 1.7×10^{12} molecules cm^{-3} per quantum state, or, assuming a rotationally equilibrated temperature of 295 K, a total singlet oxygen density of only 2.5×10^{13} molecules cm^{-3}. Further optimization of the system to further reduce detector noise is expected to reduce the minimum detectable density by a factor of three.

4. Conclusions

We have recently reported measurements of the (1,0) band of the Noxon system ($b^1\Sigma_g^+ \leftarrow a^1\Delta_g$) near 1505 nm [15]. The current measurements near 1910 nm have two key advantages over this earlier work. Most notably, the absorption cross-section of (0,0) band is almost 20 times larger than that for the (1,0) overtone. Ideally, the larger cross-section would permit the (0,0) band measurements at 1910 nm to be 20 times more sensitive than those of the (0,0) band at 1505 nm. However, due to higher detector noise and lower laser power, the (0,0) measurements are only twice as sensitive as those of the (1,0) band. A second advantage of exploiting the (0,0) band is that less reflective cavity optics may be used. In this work, we used cavity optics with 841 ppm loss at 1910 nm ($R = 99.9159\%$) compared with the 14 ppm loss optics used previously at 1505 nm ($R = 99.9986\%$) [15]. Therefore, the cavity used in the present work is more immune to extraneous cavity losses (e.g. particulates, aerosols), perhaps introducing the possibility of making in situ measurements in a COIL environment. The major drawback of working at 1910 nm is the lack of inexpensive, off-the-shelf tunable laser sources.

References

[1] W.E. McDermott, N.R. Pchelkin, D.L. Benard, R.R. Bousek, Appl. Phys. Lett. 32 (1978) 469.

[2] D.M. King, D.L. Carroll, J.K. Laystrom, J.T. Verdeyen, M.S. Sexauer, W.C. Soloman, Proceedings of the International Conference on Lasers 2000, STS Press, McLean, 2001, p. 265.

[3] M.G. Mlynczak, B.T. Marshall, Geophys. Res. Lett. 23 (1996) 657.

[4] T. Amano, K. Akao, H. Oka, O. Unno, Chem. Phys. Lett. 311 (1999) 433.

[5] S.M. Newman, I.C. Lane, A.J. Orr-Ewing, D.A. Newnham, J. Ballard, J. Chem. Phys. 110 (1999) 10749.

[6] S.M. Newman, A.J. Orr-Ewing, D.A. Newnham, J. Ballard, J. Phys. Chem. A 104 (2000) 9467.

[7] S.-L. Cheah, Y.-P. Lee, J.F. Ogilvie, J. Quant. Spectrosc. Radiat. Transfer 64 (2000) 467, Note that only the broadening term with units of m^{-1} bar^{-1} is used to estimate the pressure broadening.

[8] R.R. Gamache, A. Goldman, J. Quant. Spectrosc. Radiat. Transfer. 69 (2001) 389.

[9] H.C. Miller, J.E. McCord, J. Choy, G.D. Hager, J. Quant. Spectrosc. Ra. 69 (2001) 305.

[10] S.J. Arnold, N. Finlayson, E.A. Ogryzlo, J. Chem. Phys. 44 (1966) 2529.

[11] S.J. Davis, M.G. Allen, W.J. Kessler, K.R. McManus, M.F. Miller, P.A. Mulhall, in: OE-Lase Conf. SPIE Paper (1996) 2702.

[12] V.T. Gylys, L.F. Rubin, Appl. Opt. 37 (1998) 1026.

[13] V.S. Pazyuk, Y.P. Podmar'kov, N.A. Raspopov, M.P. Frolov, Quantum Electron. 31 (2001) 363.

[14] A.A. Frimer (Ed.), Singlet O_2 – Physical and Chemical Aspects, CRC Press, Boca Raton, FL, 1985.

[15] S. Williams, M. Gupta, T. Owano, D.S. Baer, A. O'Keefe, D.R. Yarkony, S. Matsika, Opt. Lett. 29 (2004) 1066.

[16] D.S. Baer, J.B. Paul, M. Gupta, A. O'Keefe, App. Phys. B 75 (2002) 261.

[17] A. O'Keefe, D.A.G. Deacon, Rev. Sci. Instrum. 59 (1988) 2544.

[18] L.S. Rothman, C.P. Rinsland, A. Goldman, S.T. Massie, D.P. Edwards, J.-Y. Mandin, J. Schroeder, A. McCann, R.R. Gamache, R.B. Wattsin, K. Yoshino, K.V. Chance, K.W. Juck, L.R. Brown, V. Nemtchechin, P. Varanasi, J. Quant. Spectrosc. Ra. 60 (1998) 665.

[19] Y.-N. Chiu, J. Chem. Phys. 42 (1965) 2671.

[20] L.R. Brown, C. Plymate, J. Mol. Spectrosc. 199 (2000) 166.

[21] B.J. Setzer, H.M. Pickett, J. Chem. Phys. 67 (1977) 340.

[22] J.F. Noxon, Can. J. Phys. 39 (1961) 1110.

[23] P.H. Krupenie, J. Phys. Chem. Ref. Data 1 (1972) 423.

[24] D.E. Burch, D.A. Gryvnak, Appl. Opt. 8 (1969) 1493.

[25] E.H. Fink, H. Kruse, D.A. Ramsay, M. Vervloet, Can. J. Phys. 64 (1986) 242.

[26] J.B. Tatum, Astrophys. J. Suppl. S. 16 (1967) 21.